EUROPEAN ORGANIZATION FOR NUCLEAR RESEARCH

COMPARATIVE PROPERTIES OF 400 GeV/c PROTON-PROTON INTERACTIONS

WITH AND WITHOUT CHARM PRODUCTION

LEBC-EHS Collaboration

M. Aguilar-Benitez[10], W.W.M. Allison[12], J.L. Bailly[11], S. Banerjee[3],
W. Bartl[23], M. Begalli[1], P. Beillière[6], R. Bizarri[15], H. Briand[14],
V. Canale[15], C. Caso[8], E. Castelli[22], P. Checchia[13], P.V. Chliapnikov[18],
N. Colino[10], R. Contri[8], D. Crennell[16], A. De Angelis[13], C. Defoix[6],
R. DiMarco[17], E. DiCapua[15], F. Diez-Hedo[10], J. Dolbeau[6], J. Dumarchez[14],
S. Falciano[15], C. Fisher[16]†, Yu.V. Fisyak[18], F. Fontanelli[8], J. Fry[9],
S.N. Ganguli[3], U. Gasparini[13], U. Gensch[2], S. Gentile[15], D.G. Gibaut[12],
A.T. Goshaw[7], F. Grard[11], A. Gurtu[3], R. Hamatsu[21], L. Haupt[19],
S. Hellman[19], V.P. Henri[11], J.J. Hernandez[5], S.O. Holmgren[19],
J. Hrubec[23], P. Hughes[16], D. Huss[20], M. Iori[15], E. Jegham[20],
K.E. Johansson[19], M.I. Josa[10], M. Kalelkar[17], I. Kita[21],
A.G. Kholodenko[18], E.P. Kistenev[18], S. Kitamura[21], D. Knauss[2],
V.V. Kniazev[18], W. Kowald[7], P. Ladron de Guevara[10], M. Laloum[6],
P. Legros[11], H. Leutz[5], L. Lyons[12], M. MacDermott[16], P.K. Malhotra[3],
P. Mason[9], M. Mazzucato[13], M.E. Michalon-Mentzer[20], A. Michalon[20],
T. Moa[19], R. Monge[8], L. Montanet[5], T. Naumann[2], G. Neuhofer[23],
H.K. Nguyen[14], S. Nilsson[19], H. Nowak[2], N. Oshima[21], G. Otter[1],
R. Ouared[14], J. Panella Comellas[12], G. Patel[9], G. Patrignani[15],
M. Pernicka[23], P. Pilette[11], C. Pinori[13], G. Pirreda[15], R. Plano[17],
A. Poppleton[5], P. Poropat[22], R. Raghavan[3], S. Reucroft[5], K. Roberts[9],
W.J. Robertson[7], A. Roth[1], H. Rohringer[23], J.M. Salicio[10], R. Schulte[1],
B. Sellden[19], M. Sessa[22], F. Simonetto[13], S. Squarcia[8], V.A. Stopchenko[18],
A. Subramanian[3], W. Struczinski[1], K. Takahashi[21], M.C. Touboul[14],
U. Trevisan[8], C. Troncon[22], L. Ventura[13], P. Vilain[4], C. Voltolini[20],
B. Vonck[4], W.D. Walker[7], C.F. Wild[7], T. Yamagata[21] and G. Zumerle[13]

---

† Deceased.

4002P/LM/ed

1   III. Physikalisches Institut der Technischen Hochschule, D-1500 Aachen, Federal Republic of Germany.

2   Inst. für Hochenergiephysik, AdW der DDR, DDR-1615 Berlin-Zeuthen, German Democratic Republic.

3   Tata Institute of Fundamental Research, Bombay 400005, India.

4   IIHE ULV-VUB, B-1050 Brussels, Belgium.

5   CERN, European Organization for Nuclear Research, CH-1211 Geneva 23, Switzerland.

6   Lab. de Physique Corpusculaire, Collège de France, F-75231 Paris, France.

7   Duke University, Durham, NC 27706, USA.

8   Dipartimento di Fisica and INFN, Università di Genova, I-16146 Genova, Italy.

9   Physics Department, University of Liverpool, Liverpool L693BX, UK.

10 Division of Particle Physics, CIEMAT-JEN, E-28040 Madrid, Spain.

11 Université de l'Etat à Mons, B-7000 Mons, Belgium.

12 Nuclear Physics Laboratory, University of Oxford, OX13RH, UK.

13 Dipartimento di Fisica, Università di Padova and INFN, I-35131 Padova, Italy.

14 LPNHE, Paris VI-VII, F-75231 Paris, France.

15 Dipartimento di Fisica and INFN, Università di Roma, La Sapienza, I-00185 Roma, Italy.

16 Rutherford and Appleton Laboratory, Chilton OX11OQX, UK.

17 Rutgers University, New Brunswick, NJ 08903, USA.

18 Institute for High Energy Physics, Serpukhov, SU-142284 Protvino, USSR.

19 Institute of Physics, University of Stockholm, S-11346 Stockholm, Sweden.

20 CRN Strasbourg and Université Louis Pasteur, High Energy Div.,F-67037 Strasbourg, France.

21 Tokyo University of Agriculture and Technology and Tokyo Metropolitan University, Tokyo, 158 Japan.

22 Dipartimento di Fisica and INFN, Università Trieste, I-34100 Trieste, Italy.

23 Inst. für Hochenergiephysik der Österreichischen Akademie der Wissenschaften, A-1050 Wien, Austria.

containing 425 clear charm decays, 57 decays with a charm signature but without a clear topology and 75 decays without a charm signature but paired with a charm decay in the same event.

The measurement of the charged particle multiplicity of the interactions with charm production, as well as the determination of the momentum spectrum of the hadrons accompanying (but not including) the charm hadrons, do not require a complete identification and kinematical reconstruction of the charm decays. We therefore include in this analysis all events with a "charm signature" which signals the presence of charm even if the charm decays are not unambiguously identified:

- Events with one-prong (charged particle decays) or 2-prong (neutral particle decays) not compatible with a strange particle decay (the strange particles represent, by far and large, the main source of background to charm decays in this experiment). To be incompatible with a strange particle decay, it is sufficient that at least one of the decay particles has a transverse momentum (with respect to the line of flight of the parent particle) larger than 250 MeV/c.

- Events with decay topologies (3, 4 or 5 prongs) which represent a clear signature of charm decay, even if some of the decay particles are not momentum analyzed (i.e. fall outside the spectrometer acceptance).

For the determination of the "shape" of interactions with charm production (sphericity, thrust, etc.), we need a better knowledge of the charm hadron kinematics and therefore limit ourselves to events in which at least one charm particle is completely reconstructed and identified.

3. CHARGED PARTICLE MULTIPLICITY

The charged particle multiplicity distribution observed for 400 GeV/c proton-proton interactions associated with charm production is shown in fig. 1. Charm hadrons, if charged, contribute for one unit each to this distribution (decay products, of course, are not included). To avoid the bias which could be due to hidden charm decays occurring very close to the primary vertex, we restrict the selection to events with two observed charm decays.

The charged particle multiplicity distribution observed in the same experiment for interactions with no charm production is also shown in fig. 1.

As explained in details in [1], the interaction trigger was demanding at least three hits in wire chambers placed directly downstream of LEBC, introducing a suppression of low multiplicity events. For interactions with charm production, there was a much smaller suppression since the trigger would "see", in addition to the charged particles produced at the primary interaction vertex, the charged decay products of the charm hadrons. For interactions without production of charm, the trigger efficiency was estimated by comparing the observed multiplicity distribution of ~ 600,000 interactions with the distribution derived from the KNO scaling curve of Buras et al. [3]. The parametrization

$$P_n = \frac{\psi(z)}{\langle n \rangle - 0.9} ,$$

with $z = \frac{n - 0.9}{\langle n \rangle - 0.9}$, gives a good description of proton-proton interactions in a wide energy range. The scaling curve was normalized to the data for the high values of n (n > 8) and the value of $\langle n \rangle$ = 8.99 was taken from [4]. The correction factor is large (11.1) for n = 2 but negligible for n = 8 (1.05). For interactions with charm, the correction factors were much smaller: 2.2 for n = 2, 1.075 for n = 4 and 1.014 for n = 6. The data shown in fig. 1 are corrected for these trigger losses.

The average charged particle multiplicity is $\langle n \rangle$ = 8.98 ± 0.01 for interactions without charm, the dispersion being d = 4.60 ± 0.40.

It is clear from fig. 1 that the multiplicity distributions for interactions with and without charm are different. The average charged particle multiplicity for interactions with charm is $\langle n \rangle$ = 11.0 ± 0.5, the dispersion being d = 3.9 ± 0.2.

The increase in $\langle n \rangle$, going from interactions without charm to those with charm, is about two units. The significance of this observation may perhaps be better appreciated by noting that such an increase of $\langle n \rangle$ corresponds to the change of average multiplicity when going from 400 GeV/c to 1060 GeV/c proton-proton interactions [5].

4. LONGITUDINAL AND TRANSVERSE MOMENTUM DISTRIBUTIONS OF THE PIONS IN CHARM EVENTS

To reduce the contamination due to misidentified leading protons, we limit the analysis to negatively charged particles and reject from this sample the tracks which, according to the particle identification provided by EHS, have a larger probability to be a K^- or a $\bar{p}$. Tracks for which no particle identification is available are taken as pions.

The relative longitudinal momentum x (0 < x < 1) and p_T^2 distributions of π^- are shown in figs 2(a) and 2(b), respectively. The invariant longitudinal momentum spectrum is rather soft, as expected for central production. A fit with the function

$$E^* \frac{dN}{dx} \propto (1 - x)^n$$

yields n = 5.2 ± 0.5. This result underlines the softer behaviour of these pions with respect to those observed for interactions without charm production. In this last case, n = 4.0 for a rather large range of incident momentum [6]. This is also the value predicted by the quark counting rules [7].

The transverse momentum squared distribution follows a double exponential behaviour, with a large slope (exp $(-10.6\ p_T^2)$ at small p_T^2 followed by a smaller one above $p_T^2 = 0.20$ (GeV/c)^2 : exp$(-4.6\ p_T^2)$. The average transverse momentum is 326 ± 9 MeV/c, to be compared to 334 ± 3 MeV/c for 360 GeV/c proton-proton interactions [8] or to 352 ± 5 MeV/c for 405 GeV/c proton-proton interactions [9].

5. EVENT SHAPE IN MOMENTUM SPACE

The shape of the events in momentum space is analyzed in terms of sphericity and thrust [10]:

$$S = \frac{3}{2} \min \frac{\sum p_T^2}{\sum p^2}$$

$$T = \max \frac{\sum |p_{/\!/}|}{\sum p}$$

where p_T and $p_{/\!/}$ refer to the transverse and longitudinal momentum of the secondaries, respectively, with respect to an arbitrary direction in the centre of mass system. When the minimum (for S) or the maximum (for T) is reached, this direction defines the main axis of the event. This axis is very close to the direction of the incident beam particle in our case. The observed trends of S and $1 - T$ for e^+e^-, lepton hadron, hard and soft hadronic interactions [11] is to steadily decrease with increasing total energy, indicating the dominance of two jet final states. The trend evolves into larger sphericities observed for e^+e^- annihilations above ~ 25 GeV, a new feature attributed to the presence of 3-jet events, whereas such an evolution is not observed for soft hadron interactions at similar energies [12].

S and T have been calculated for all events with, at least, one reconstructed charm particle and having at least one non charm charged particle emitted in the forward c.m.s. hemisphere. Such a selection is in agreement with the symmetric behaviour of proton-proton interactions and takes into account EHS acceptance. This selection does not affect T, whereas Monte-Carlo simulations have shown that the corrections on S due to this selection are smaller than statistical errors on this quantity. The sample used for our calculations consists of 101 events with charm production. After correcting for charm visibility, acceptance losses and kinematical ambiguities, one finds the average values:

$$\langle S \rangle = 0.14 \pm 0.02.$$
$$\langle 1 - T \rangle = 0.12 \pm 0.01.$$

The reliability of these results was checked, repeating the calculations for samples of events having at least 2, 3, 4, 5 particles emitted in the forward c.m.s. hemisphere: no significant deviation from the quoted values were found.

We also checked that the reconstruction inefficiency (4% for charge particles emitted in the forward c.m.s. hemisphere) had negligible effects on $\langle S \rangle$ and $\langle 1 - T \rangle$.

The mean values obtained for S and $1 - T$ for 360 GeV/c proton-proton non-diffractive interactions without charm production are very similar [12]:

$$\langle S \rangle = 0.136 \pm .003,$$
$$\langle 1 - T \rangle = 0.120 \pm 0.002.$$

The charge multiplicity dependence of $\langle S \rangle$ and $\langle 1 - T \rangle$ is shown in fig. 3. Both quantities increase with the number of charged particles, as also observed for soft hadronic interactions (70 GeV/c K^+p interactions [13], 147 GeV/c (π^+, K^+, p)p interactions [14]). The rise of $\langle S \rangle$ and $\langle 1 - T \rangle$ with increasing multiplicity is very steep in soft hadronic interactions where the production of additional particles leads to more and more isotropy. A weaker dependence is observed for events with charm production. This production, characterized by relatively large p_T values for the charm particles, has a clear influence on the event shape. More quantitatively, one obtains $\langle S \rangle = 0.110 \pm 0.014$, $\langle 1 - T \rangle = 0.097 \pm 0.006$ for events with charm particles produced at $p_T < 1$ GeV/c, whereas $\langle S \rangle = 0.200 \pm 0.025$, $\langle 1 - T \rangle = 0.166 \pm 0.012$ if $p_T > 1$ GeV/c.

In fig. 3, the data are also compared to model predictions. For these predictions, one combines the charm quark generating process.

$$gg \to c\bar{c}$$

(where g denotes hard gluons) with the Lund fragmentation scheme [15]. With this ensatz, the multiplicity dependence of $\langle S \rangle$ and $\langle 1 - T \rangle$ is fairly well reproduced.

Fig. 4 shows a comparison of the event shape $\langle 1 - T \rangle$ and the average charged multiplicity for interactions with and without charm production. The non-charm production data cover a large range of incident momentum (10 to 400 GeV/c) and initial states ($\pi^\pm p$, $K^\pm p$, pp interactions) [12-14, 16]. For non-diffractive production, the multiplicities were estimated, if not published, using the approximation suggested by Wroblewski [17]. The point corresponding to events with charm production (this experiment) lies above the general trend observed for soft hadronic interactions. This is primarily due to larger multiplicities observed for events with charm production.

6. SUMMARY

The global properties of 400 GeV/c proton-proton interactions with charm production have been studied.

The comparison of these properties to those of soft hadronic interactions at similar energies shows an increase of the mean charged particle multiplicity and a softening of the momentum spectra for the hadrons (pions) produced in association with charm.

It is natural to interpret these differences by the more central nature of collisions leading to charm production. The mean charged particle multiplicity of the interactions with charm production is $\langle n \rangle = 11.0 \pm 0.5$, about two units larger than for soft hadronic processes and the relative longitudinal momentum dependence of the negative pions follows the distribution $(1 - x)^{5.2}$ whereas it is $(1 - x)^4$ for normal hadronic production.

The increase of $\langle S \rangle$ and $\langle 1 - T \rangle$ with the charged particle multiplicity of the final state is fairly well reproduced by a QCD fusion model combined with the Lund fragmentation scheme.

Analyzing the dependence of the event shape on the average multiplicity one finds that charm final states are more spherical than expected from the general trend observed for the various soft hadron experiments. A simple explanation is that charm events are less collinear due to the high transverse momentum of the charm particles and due to the larger multiplicities of the final states.

REFERENCES

[1] M. Aguilar-Benitez et al., Nucl. Instr. & Meth. A258 (1987) 26.

[2] M. Aguilar-Benitez et al., To be published in Z. Phys. C (1988).

[3] A. Buras et al., Phys. Lett. 47B (1973) 251.

[4] C. Bromberg et al., Phys. Rev. Lett. 31 (1973) 1563.

[5] A. Breakstone et al., Phys. Rev. D30 (1984) 528.

[6] R.T. Edwards, Phys. Rev. D18 (1978) 76;
     D. Cutts et al., Phys. Rev. Lett. 43 (1979) 319;
     D. Denegri et al., Phys. Lett. 98B (1981) 127.

[7] J.F. Gunion, Phys. Lett. 88B (1979) 150.

[8] C. Bromberg et al., Nucl. Phys. B107 (1976) 82.

[9] J.L. Bailly et al., Z. Phys. C35 (1987) 295.

[10] S. Brandt and H.D. Dahmen, Z. Phys. C1 (1979) 61.

[11] W. Kittel, Low p_T - soft collisions in the light of hard
     collisions, Proceedings of the XVIth Symp. on Multiparticle
     Dynamics, Kiryat Anavim (1985).

[12] J.L. Bailly et al., Phys. Lett. B, to be published (1988).

[13] M. Barth et al., Nucl. Phys. B192 (1981) 289.

[14] D. Brick et al., Z. Phys. C15 (1982) 1.

[15] B. Andersson, H.U. Bengtsson and G. Gustavsson, Charm production
     in the confining force field, LU TP 83/4, Lund 1983;
     T. Sjostrand, The Lund Monte-Carlo for jet fragmentation, Computer
     Physics Communications 27 (192) 243.
     M. Aguilar-Benitez et al., Phys. Lett. B189 (1987) 476.

[16] R. Göttgens et al., Nucl. Phys. B178 (1981) 392.

[17] A. Wroblewski, Hadronic multiplicities and correlations, Universality
     of Hadron Production?, Proc. of the XIVth Symposium on Multiparticle
     Dynamics, Lake Tahoe (1983).

FIGURE CAPTIONS

Fig. 1   Charged particle multiplicity distributions, for 400 GeV/c
         proton—proton interactions with and without charm production.
         The data shown are corrected for trigger losses. The KNO
         scaling curve, with Buras' parametrization, is also shown (see
         text).

Fig. 2   Momentum distributions of negative pions emitted in the forward
         c.m.s. hemisphere from events with charm production:

         (a) Invariant relative longitudinal x distribution.
         (b) p_T^2 distribution.

Fig. 3   Dependence of the sphericity and thrust on the charged particle
         multiplicity of the final states for interactions with charm
         production. The corresponding distributions for 70 GeV/c and
         147 GeV/c interactions without charm production are also shown.
         QCD model predictions are also shown (see text).

Fig. 4 $\langle 1 - T \rangle$ versus the mean charged particle multiplicity observed
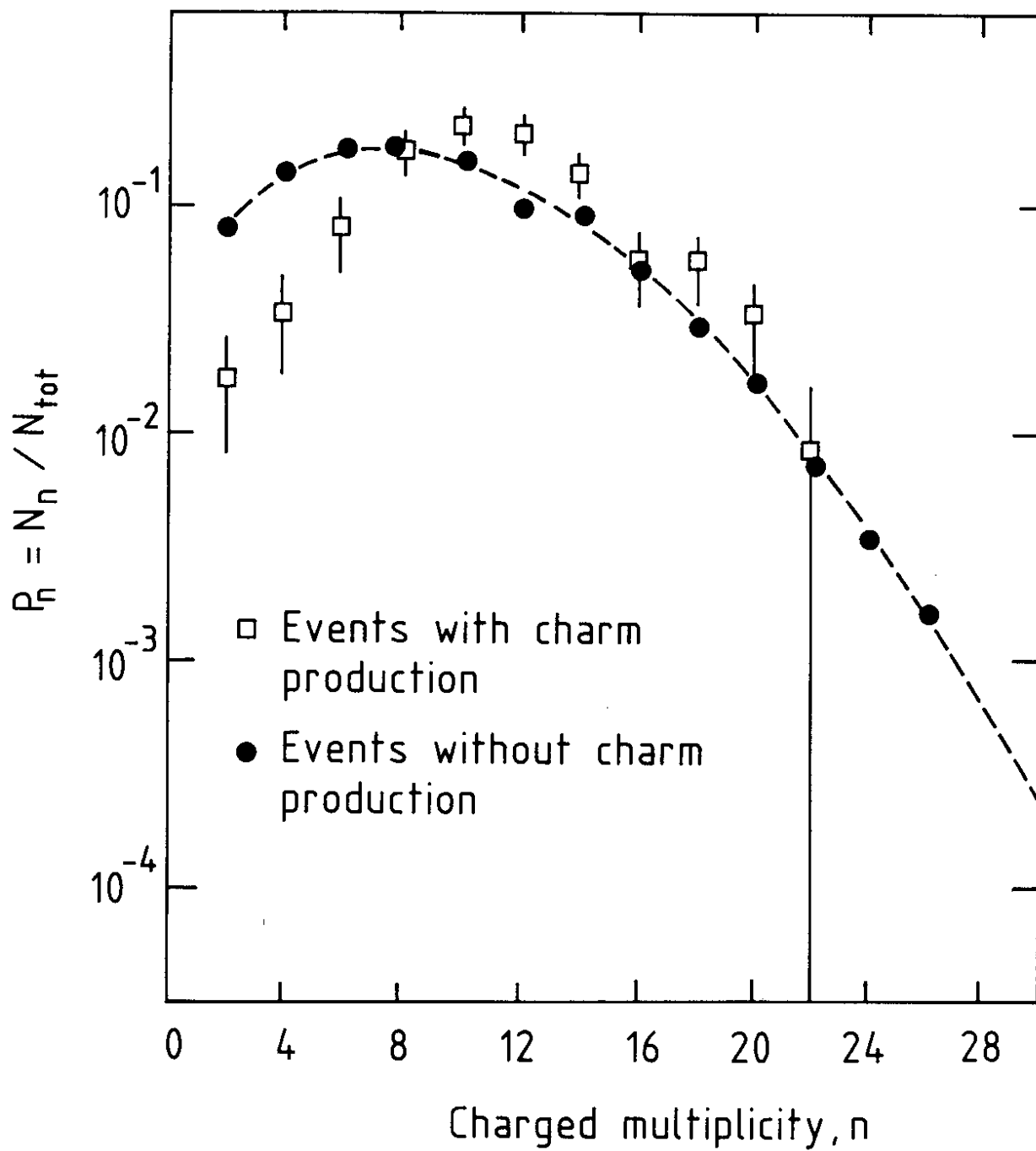   for this experiment (with charm production) and others (without
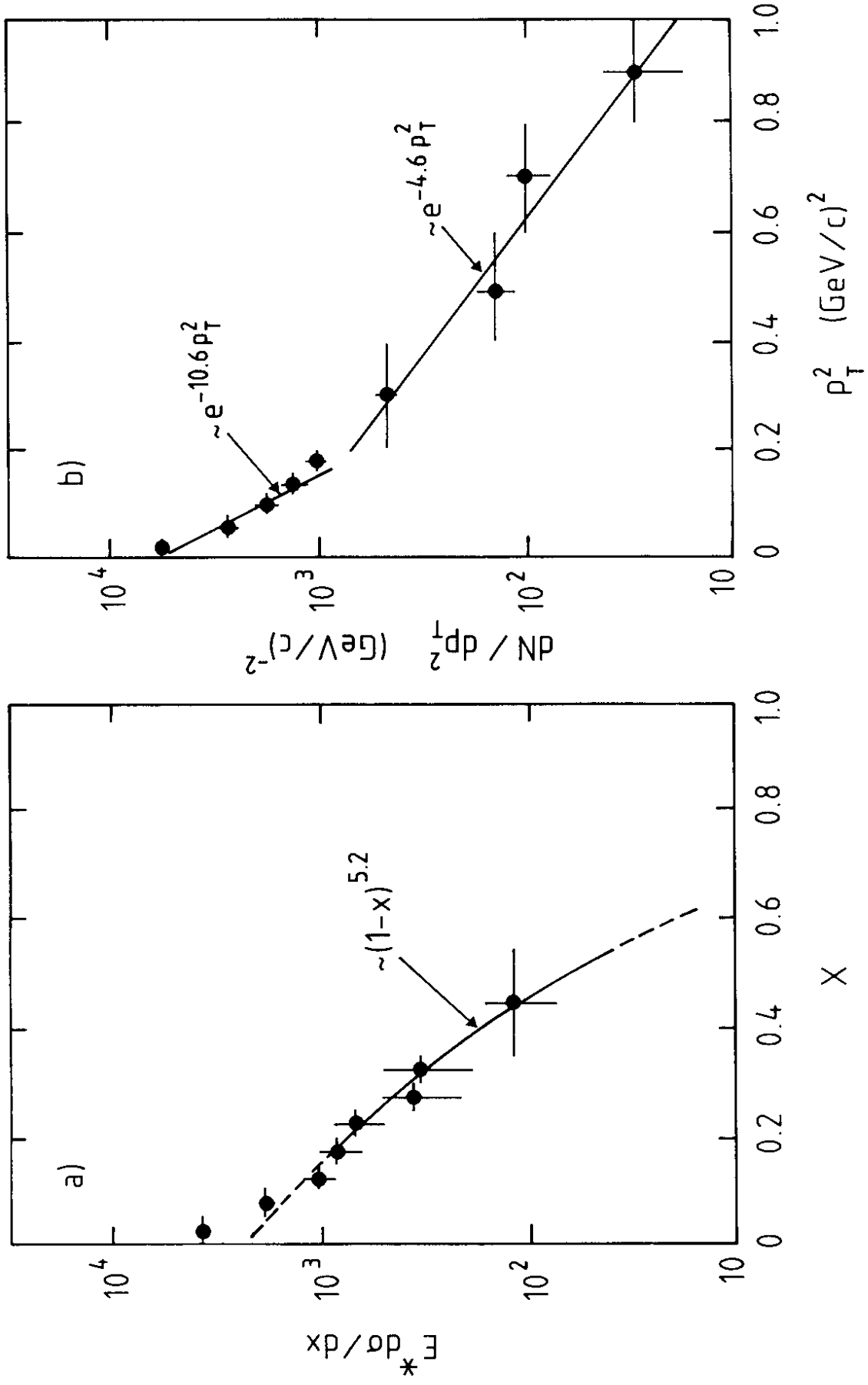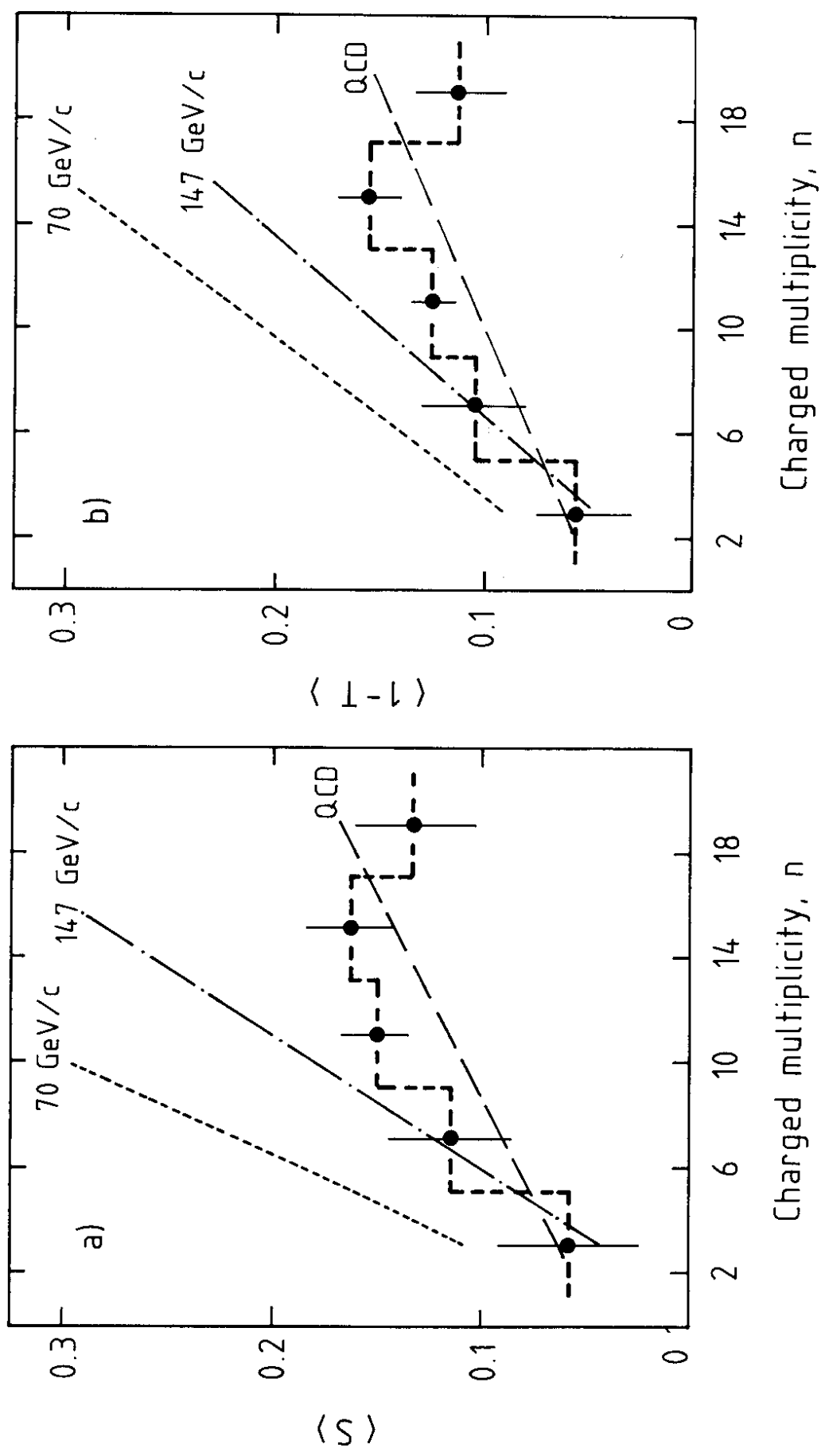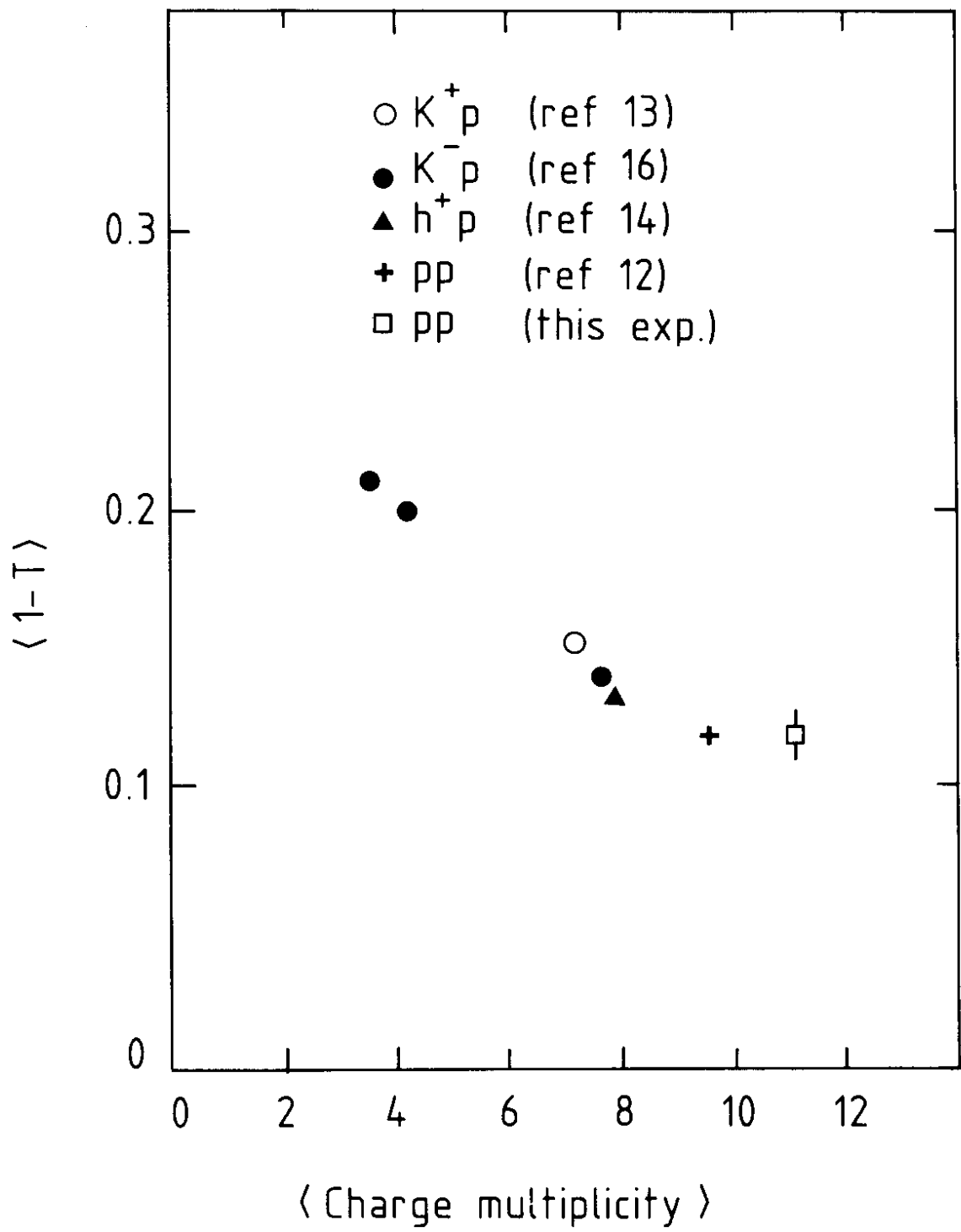   charm production).

FIG. 1

FIG. 2

FIG. 3

FIG. 4